On the development of high temperature ammonia-water hybrid absorption-compression heat pumps

Jensen, Jonas Kjær; Markussen, Wiebke Brix; Reinholdt, Lars; Elmegaard, Brian

Published in:
International Journal of Refrigeration

Link to article, DOI:
10.1016/j.ijrefrig.2015.06.006

Publication date:
2015

Document Version
Peer reviewed version

On the development of high temperature ammonia-water hybrid absorption-compression heat pumps

Jonas K. Jensen[a,*], Wiebke B. Markussen[a], Lars Reinholdt[b], Brian Elmegaard[a]

[a]*Technical University of Denmark, Department of Mechanical Engineering, Nils Koppels Alle, Building 403, DK - 2800, Kgs. Lyngby, Denmark*
[b]*Danish Technological Institute, Kongsvang Alle 29, DK-8000 Aarhus, Denmark, Denmark*

Abstract

Ammonia-water hybrid absorption-compression heat pumps (HACHP) are a promising technology for development of efficient high temperature industrial heat pumps. Using 28 bar components HACHPs up to 100 °C are commercially available. Components developed for 50 bar and 140 bar show that these pressure limits may be possible to exceed if needed for actual applications. Feasible heat supply temperatures using these component limits are investigated. A feasible solution is defined as one that satisfies constraints on the COP, low and high pressure, compressor discharge temperature, vapour water content and volumetric heat capacity. The ammonia mass fraction and the liquid circulation ratio both influence these constraining parameters. The paper investigates feasible combinations of these parameters through the use of a numerical model. 28 bar components allow temperatures up to 111 °C, 50 bar up to 129 °C, and 140 bar up to 147 °C. If the compressor discharge temperature limit is increased to 250 °C and the vapour water content constraint is removed, this becomes: 182 °C, 193 °C and 223 °C.

Keywords: High temperature heat pump, industrial heat pump, absorption-compression, ammonia-water

1. Introduction

The hybrid absorption-compression heap pump (HACHP), or vapour compression heat pump with solution circuit is based on the Osenbrück cycle (Osenbrück, 1895). In the Osenbrück cycle the processes of condensation and evaporation are exchanged with absorption and desorption processes. It thus uses zeotropic mixtures as the working fluid, typically ammonia-water.

The first theoretical study of the HACHP was performed by Altenkirch (1950) and describes the advantage of the HACHP with the non-isothermal process of absorption-desorption compared to the isothermal process of condensation-evaporation in a conventional vapour compression heat pump (VCHP). Thereby the HACHP cycle approaches the Lorenz cycle (Lorenz, 1894), which can result in an increased COP due to the reduction of entropy generation driven by heat transfer over a finite temperature difference. The efficiency advantage of the HACHP over the VCHP requires the temperature change (glide) in the heat sink and heat source to be greater than 10 K (Berntsson and Hultén, 2002). The advantage remains even if economic considerations are included in the comparison (Berntsson and Hultén, 1999). This makes the HACHP a relevant technology for industrial heat supply and waste heat recovery as these processes often require large sink-source temperature glides.

A further advantage of using a zeotropic mixture as working fluid is the reduction of vapour pressure compared to the vapour pressure of the pure volatile component. This implies that the HACHP can achieve higher supply temperatures than a VCHP at the same working pressure. The HACHP is thus, of specific interest for high temperature applications. Brunin et al. (1997) showed that it is technically and economically feasible to use the HACHP up to a heat supply temperature of 140 °C, this however is based on a high pressure constraint of 20 bar corresponding to the limitations of standard refrigeration components at the time of the study. In the meantime new compressor types such as high pressure NH_3 (50 bar) and transcritical CO_2 (140 bar) have become commercially available and further standard refrigeration components now operate at 28 bar. It is therefore of interest to evaluate how the application of these components changes the working domain of the HACHP.

One design constraint that is not discussed in the study by Brunin et al. (1997) is the compressor discharge temperature. However, most compressor manufacturers require this to be lower than 180 °C (Nekså et al., 1998). This is mainly due the thermal stability of the lubricating oil and the thermal stress of the materials surrounding the compressor discharge line. This is mainly an issue for reciprocating compressors. Changing the lubricant from a mineral oil to synthetic oil could relax the constraint due to thermal stability. This however requires that a synthetic oil that meets the requirements of miscibility etc. is identified. Adjustments to the gasket materials and alike could also make the compressor durable at higher discharge temperatures. It is assumed to be a realistic estimate that compressor discharge temperatures up to 250 °C can be sustained with minor adjustments.

To evaluate the working domain of the HACHP using the recently developed high pressure equipment a set of design con-

*Corresponding author
Email addresses: jkjje@mek.dtu.dk (Jonas K. Jensen), wb@mek.dtu.dk (Wiebke B. Markussen), lre@teknologisk.dk (Lars Reinholdt), be@mek.dtu.dk (Brian Elmegaard)

Nomenclature

COP Coefficient of Performance (-)
f Circulation ratio (-)
$\dot{m}$ Mass flow rate (kg s^{-1})
p Pressure (bar)
PR Pressure ratio p_H/p_L (-)
q Vapour mass fraction (-)
$\dot{Q}$ Heat rate (kW)
T Temperature (°C)
ΔT Temperature difference (K)
v Specific volume (m^3 kg^{-1})
$\dot{V}$ Volume flow rate (m^3 s^{-1})
VHC Volumetric heat capacity (MJ m^{-3})
$\dot{W}$ Power (kW)
x Ammonia mass fraction (-)

Abbreviations
EES Engineering Equation Solver
HACHP Hybrid absorption compression heat pump
IHEX Internal Heat Exchanger
VCHP Vapour compression heat pump

Greek letters
ε Heat exchanger effectiveness
η Efficiency

Subscripts
AB Absorber
CM Compressor
DS Desorber
dis Displacement
e Electrical
GC Gas cooler
H High
IH Internal heat exchanger
is Isentropic
l Lean
L Low
pp Pinch point
r Rich
suc Suction
v Vapour
vol Volumetric

straints are defined. A solution that satisfies this set of constraints will constitute an economically and technically feasible solution. The technical limitations are: the high pressure, governed by the choice of compressor technology, the low pressure, set to eliminate entrainment of air, and the compressor discharge temperature, as discussed above. Further, for the ammonia compressors a constraint is set on the vapour ammonia mass fraction. The economic constraints are: the Coefficient of Performance (COP) and the volumetric heat capacity (VHC), calculated as the ratio of the compressor displacement volume to the heat output of the HACHP (Brunin et al., 1997).

Two design parameters influence the design values of the constraining parameters significantly. These are the rich ammonia mass fraction, x_r, and the circulation ratio, f, defined as the ratio between the mass flow rate of the rich solution and the lean solution. The combination of these two govern the system pressure and thereby the VHC. Also the slope of the absorption-desorption curve and thereby the performance (COP) is influenced by these parameters. These relations have been addressed with different approaches by Stokar and Trepp (1987), Åhlby et al. (1991), Rane and Radermacher (1992), Rane et al. (1993), Berntsson and Hultén (1999, 2002) and latest by Zamjlrescu (2009).

The present study investigates the set of feasible combination of x_r and f at heat supply temperatures of 100 °C, 125 °C, 150 °C and 175 °C. Working domains will be evaluated for all three mentioned types of refrigeration components.

2. Method

2.1. The HACHP process

The process diagram of the evaluated HACHP is seen in Fig. 1a. The working principle of the HACHP is as follows. At the outlet of the desorber the working fluid is a liquid-vapour mixture. The liquid phase will have a lean concentration of ammonia, while the vapour phase consists primarily of ammonia (at low pressures the vapour water content can be substantial). The bulk ammonia concentration of the stream exiting the desorber is the rich ammonia mass fraction.

Before elevating the pressure the vapour and liquid phases must be separated such that liquid does not enter the compressor. This is done in the liquid-vapour separator placed after the desorber. The vapour is drawn from the top of the tank to the compressor in which the pressure and temperature are increased. Next the vapour passes to the gas cooler in which the vapour temperature is reduced, while releasing heat to the sink. The lean liquid is drawn from the bottom of the separator tank to the pump where the pressure is elevated to the high pressure. As the liquid is close to incompressible the temperature increase over the pump is small. Therefore, the liquid is heated in the internal heat exchanger (IHEX). This reduces the entropy generation when mixing the liquid and vapour at the high pressure.

Prior to the absorber the vapour and liquid phases are mixed in an adiabatic process which results in a vapour-liquid mixture in thermal, mechanical and chemical equilibrium. In a physical system this would not be a separate component, but the adiabatic absorption process would takes place in the first part of the absorber. In a thermodynamic model both treatments yield

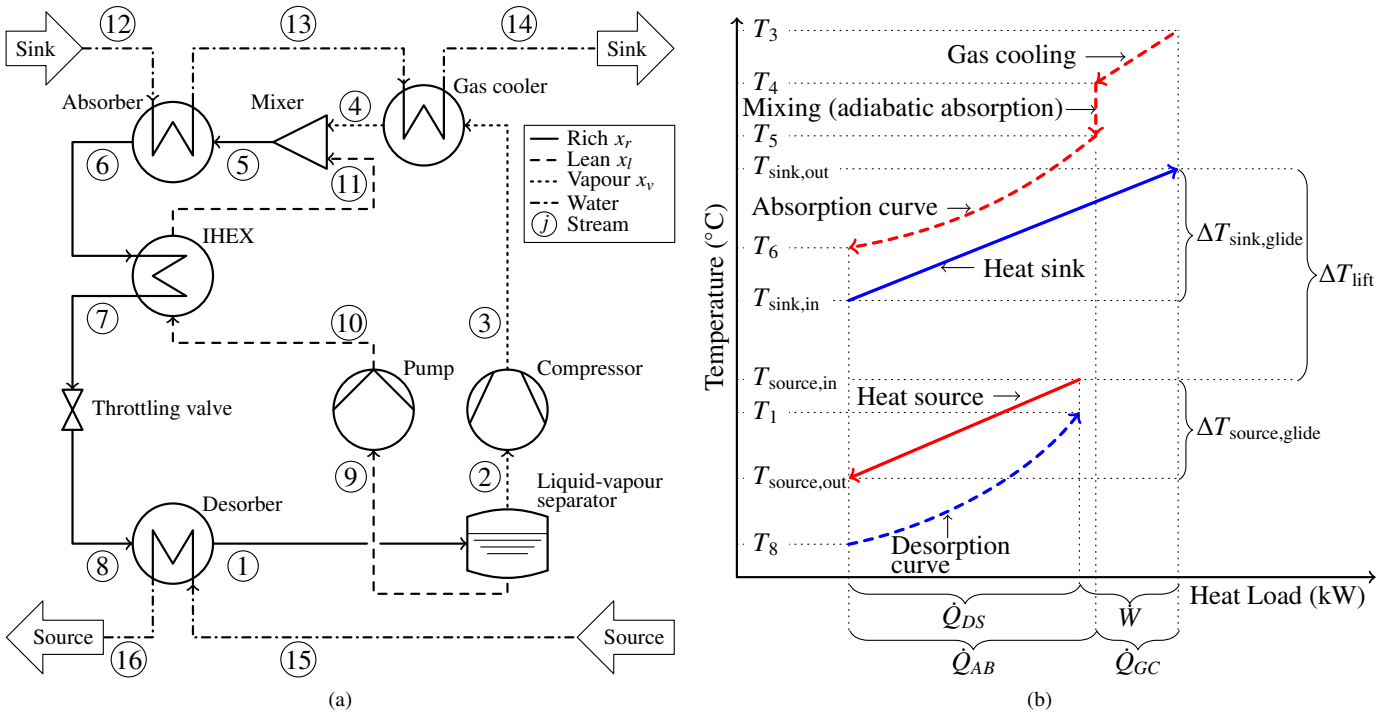

Figure 1: (a) Principle sketch of the HACHP, (b) HACHP process sketched in a temperature - heat load diagram

the same result. When thermodynamic equilibrium is reached the diabatic absorption process begins. Here the ammonia is absorbed in the lean liquid solution while releasing heat to the sink

At the absorber outlet a saturated liquid rich in ammonia is delivered. This is sub-cooled in the IHEX. The sub-cooled rich ammonia solution is throttled to the low pressure resulting in a low temperature liquid-vapour mixture. This is fed to the desorber in which vapour is generated by supplying heat from the source.

The process described above is sketched in the temperature – heat load diagram shown in Fig. 1b. Here the temperature lift, ΔT_{lift}, is defined as the difference between the sink outlet temperature (heat supply temperature) and the source inlet temperature. The temperature glide, ΔT_{glide}, is defined as the temperature difference between the inlet and outlet of the sink and source, respectively. Further, it is seen that the profiles of the absorption and desorption processes are non-linear. This has been described in detail by Itard and Machielsen (1994). In Fig. 1b these processes are depicted as convex curves. Depending on the ammonia mass fraction and circulation ratios these profiles could also exhibit a concave curve or have a convex and a concave part. This is well described in Zheng et al. (2013). Thus, when modelling the HACHP it is not sufficient to use a lumped parameter model of the component to ensure a positive temperature difference at the inlet and outlet of the absorber and desorber. To ensure a feasible profile it is necessary to use a distributed model and verify that there is a positive temperature difference over the entire heat transfer process.

Table 1: Component inputs to the thermodynamic model

Component	Input	Value	Unit
Compressor	η_{is}	0.75	(-)
Compressor	η_{vol}	0.90	(-)
Compressor	η_{e}	0.90	(-)
Pump	η_{is}	0.75	(-)
Pump	η_{e}	0.90	(-)
Gas cooler	ε	0.85	(-)
Absorber	ΔT_{pp}	5.00	(K)
IHEX	ε	0.85	(-)
Desorber	ΔT_{pp}	5.00	(K)

Table 2: External operating conditions

ΔT_{sink}	20	K
ΔT_{lift}	25	K
$\dot{m}_{\text{sink}}$	1	kg s^{-1}
$\dot{m}_{\text{source}}$	2	kg s^{-1}

2.2. *Thermodynamic modelling of the HACHP heat pump*

A numerical model of a HACHP has been developed in MATLAB 2015a (2015). The thermodynamic properties of the ammonia-water mixture were calculated using the REFPROP 9.1 (2013) interface for MATLAB. The so called 'Ammonia (Lemmon)' formulation was applied. As discussed in Modi and Haglind (2015) this formulation significantly increases the robustness of the property calculations compared to the default Tillner-Roth and Friend (1998) formulation, especially in the two-phase region. The robustness is achieved without signifi-

cantly compromising the accuracy of the property calculations (Modi and Haglind , 2015).

Each component was modelled based on steady state mass and energy balances. Further, the model ensured that the second law of thermodynamics is fulfilled in all components.

Heat losses from components and pressure losses were neglected. The rich ammonia mass fraction, x_r, and circulation ratio, f, were inputs to the model. The rich ammonia mass fraction was present in state 5-8 and 1. The circulation ratio was defined as the ratio between the mass flow rate of the rich solution, $\dot{m}_r$, and the lean solution, $\dot{m}_l$, see Eq. (1). Hence, the circulation ratio was directly linked to the vapour quality in state 1 exiting the desorber, such that: $q_1 = 1 - f$. From this it can be concluded that if the circulation ratio is 0 then the HACHP is in principle a VCHP with a zeotropic working fluid.

$$f = \frac{\dot{m}_l}{\dot{m}_r} \tag{1}$$

As pressure and heat losses were neglected the temperature and pressure in the liquid-vapour separator were the same as that exiting the desorber. It was assumed that the vapour and liquid exiting the desorber were saturated, $q_2 = 1$ and $q_9 = 0$. The vapour and lean ammonia mass fraction, x_v and x_l, were then determined.

The processes in the compressor and pump were modelled as adiabatic with given isentropic efficiencies, η_{is}. The transferred heat in the IHEX and gas cooler were calculated based on given values of heat exchanger effectiveness, ε. The mixing or adiabatic absorption process found prior to the absorber was modelled only by a mass and energy balance. Thus, state 5 was the equilibrium state attained when mixing stream 4 and 11. The state exiting the absorber was assumed to be saturated, $q_6 = 0$. The expansion in the throttling valve was assumed to be isenthalpic, $h_7 = h_8$.

The high and low pressures, p_H and p_L, were determined to satisfy given values of pinch point temperature difference, ΔT_{pp}, in the absorber and desorber. As enthalpy and temperature are not proportional during absorption and desorption, the absorber and desorber were discretised in heat load, giving the specific enthalpy of both the sink-source and ammonia-water mixture at each step. Assuming constant pressure and constant bulk ammonia mass fraction the equilibrium temperatures and temperature differences were attained at each step. The pinch point temperature difference is defined as the minimum of these temperature differences. 40 steps were used in this model for both the absorber and desorber.

The COP of the HACHP was defined as given in Eq. (2). Here $\dot{W}_{\text{CM}}$ and $\dot{W}_{\text{PM}}$ were the work calculated based on the given isentropic efficiencies. The efficiency of the electric motors driving the pump and compressor was accounted for by the electric efficiency, η_e.

$$\text{COP} = \frac{\dot{Q}_{\text{AB}} + \dot{Q}_{\text{GC}}}{\frac{\dot{W}_{\text{CM}}}{\eta_{e,\text{CM}}} + \frac{\dot{W}_{\text{PM}}}{\eta_{e,\text{PM}}}} \tag{2}$$

The displacement volume of the compressor, $\dot{V}_{\text{dis}}$, was found by Eq. (3), here $\dot{V}_{\text{suc}}$ was the suction line volume flow rate, η_{vol} was the volumetric efficiency of the compressor and v_2 was the specific volume of state 2.

$$\dot{V}_{\text{dis}} = \frac{\dot{V}_{\text{suc}}}{\eta_{\text{vol}}} = \frac{\dot{m}_2 v_2}{\eta_{\text{vol}}} \tag{3}$$

The VHC was calculated as the ratio between the heat output of the HACHP and the displacement volume of the compressor, see Eq. (4). VHC was thus a measure of the size of compressor needed to deliver a certain heat load.

$$\text{VHC} = \frac{\dot{Q}_{\text{AB}} + \dot{Q}_{\text{GC}}}{\dot{V}_{\text{dis}}} \tag{4}$$

The pinch point temperature difference of the absorber and desorber, the isentropic, volumetric and electrical efficiencies of the compressor and pump and the effectiveness of the IHEX and gas cooler were fixed parameters. The applied values are listed in Table 1. Further, the operating conditions, constituted by ΔT_{sink}, ΔT_{source}, $\dot{m}_{\text{sink}}$ and $\dot{m}_{\text{source}}$ were fixed inputs to the model, these values are stated in Table 2.

Table 3: Design constraints for standard refrigeration, high pressure NH_3 and transcritical CO_2 components

	Unit	Standard ref.	High pressure NH_3	Transcritical CO_2
$p_{H,\text{max}}$	bar	28	50	140
$p_{L,\text{min}}$	bar	1	1	1
$T_{H,\text{max}}$	°C	170	170	250
COP_{min}	-	4	4	4
VHC_{min}	MJ m^{-3}	2	2	2
$x_{v,\text{min}}$	-	0.95	0.95	0.00

2.3. Design constraints

The design constraints are listed in Table 3. The constraint on COP and VHC ensures the economic feasibility of the heat pump as a high COP ensures a low running cost and a high VHC ensures a low investment cost. The applied values for the COP and VHC constraint are set in agreement with those presented by Brunin et al. (1997). Here the constraint on the low pressure is also presented. This was set to 1 bar to prevent sub-atmospheric pressures and thus removes the risk of air entrainment. The high pressure constraints for the different compressor technologies are summarized by Ommen et al. (2011).

For the two ammonia compressors a constraint was imposed on the vapour ammonia mass fraction, x_v. It was assumed that 5% water is acceptable in an ammonia compressor. For the modified transcritical CO_2 compressor no constraint was imposed on x_v as they may just as well be modified to handle the needed ammonia-water composition.

Nekså et al. (1998) states that compressor discharge temperatures up to 180 °C should be possible without degeneration of lubricant, while Ommen et al. (2011) state this could be as low as 160 °C. The value for the unmodified compressors was set to 170 °C in this study. For the modified transcritical CO_2 components, 250 °C was chosen as previously discussed.

3. Results

The design of the HACHP has two more degrees of freedom compared the VCHP. The design of a VCHP can be determined using the component inputs from Table 1 and the external operating conditions: $\Delta T_{\text{sink,glide}}$, ΔT_{lift}, $T_{\text{sink,out}}$, $\dot{m}_{\text{sink}}$ and $\dot{m}_{\text{source}}$. For the HACHP the circulation ratio, f, and the ammonia mass fraction, x_r, must also be given. Hence, it is of relevance to investigate how the choice of these inputs influence the design of the HACHP.

3.1. Influence of x_r and f

Fig. 2 shows COP, VHC, compressor discharge temperature, T_H, high pressure, p_H, low pressure, p_L and vapour ammonia mass fraction, x_v for the HACHP. The component inputs, listed in Table 1, and the external operating conditions, listed in Table 2, were held constant. The heat supply temperature was, $T_{\text{sink,out}}$ = 100 °C. The calculations were carried out for x_r and f ranging from 0.1 to 0.9 in steps of 0.025. As the constrained parameters are independent of the heat load the presented results are valid for all HACHPs in which the sink-source mass flow ratio is $\dot{m}_{\text{sink}}/\dot{m}_{\text{source}}$ = 0.5.

When comparing the contours of the high and low pressure it becomes evident that the circulation ratio has a greater influence on the low pressure than on the high pressure. The circulation ratio only influences the high pressure at high ammonia mass fractions and high circulation ratios. The low pressure is governed by both parameters such that an increase in ammonia mass fraction and an increase in circulation ratio will increase the low pressure. Thus, the lowest low pressure is found at x_r = 0.1, f = 0.1 and the highest low pressure is at x_r = 0.9, f = 0.9. From this it is apparent that a set of combinations induce a significant increase in the system pressure ratio (PR), see Fig. 3. These are combinations with low circulation ratio and ammonia mass fractions around 0.5. This further induces a large increase in compressor discharge temperature varying from 150 °C for the low pressure ratio combinations to 450 °C in the high pressure ratio range.

The increased pressure ratio and compressor discharge temperature also have a significant influence on the COP. As seen, the COP contours resemble those of the pressure ratio and compressor discharge temperature. The COP is greatly reduced for the combinations with high pressure ratios as the increased compressor discharge temperature increases the entropy generation in the gas cooler and mixer due to the very large temperature differences. It is seen that for all ammonia mass fractions one circulation ratio exists that optimizes the COP. This is indicated by the dashed line marked COP_{max}. For circulation ratios above this optimum line the COP drops although the pressure ratio is reduced. As seen, the higher the ammonia mass fraction, the lower the optimal circulation ratio.

The VHC is directly influenced by the specific volume in the suction line and thus the low pressure governs this parameter. This is apparent when comparing the contours of the VHC and low pressure. Further, it is seen that also the vapour ammonia mass fraction is linked to the low pressure. As seen, the lower the pressure the lower the vapour ammonia mass fraction.

All important design parameters are greatly influenced by both ammonia mass fraction and circulation ratio and thus the behaviour of these cannot be attributed solely to one of the two. Thus, the main conclusion derived from Fig. 2 is that the correct combination of ammonia mass fraction and circulation ratio is needed in order to identify a feasible design.

3.2. Feasible design combination of x_r and f

In order to evaluate the applicability of the HACHP for high temperature concepts ($T_{\text{sink,out}}$>100 °C) the feasible combinations of ammonia mass fraction and circulation ratios must be identified in this temperature range. The feasible design combinations are given by the design constraints listed in Table 3. As these are specific to the three technologies (standard, high pressure NH_3 and transcritical CO_2) three sets of feasible combinations exist.

These sets of feasible combinations have been analysed at four heat supply temperatures $T_{\text{sink,out}}$ = 100 °C, 125 °C ,150 °C and 175 °C. Again the component inputs from Table 1 and the external operating conditions from Table 2 were kept constant.

Fig. 4 shows the feasible combinations of the three technologies at the four heat supply temperatures. Fig. 4 (a) shows this for $T_{\text{sink,out}}$ = 100 °C. As seen a feasible set of combinations exist for all three technologies. The set belonging to the standard refrigeration components is the smallest of the three and is constrained by the high pressure, p_H, and compressor discharge temperature, T_H. The set belonging to the high pressure NH_3 technology is significantly larger than that of the standard components. This set is constrained by p_H, T_H and COP. The largest set is that of the transcritical CO_2 components constraints. This set is constrained by the VHC, T_H and COP. Further, it can be noted that the x_v constraint is dominant over both the low pressure and VHC constraint in the entire range, thus these constraints are effectively extraneous.

In Fig. 4 (b) the heat supply temperature is increased to 125 °C. As seen, this has the consequence that the high pressure constraint for the standard components moves beyond the compressor discharge temperature constraint deeming the application of the standard refrigeration components infeasible. A small set of feasible combinations exist for the high pressure NH_3 components. This set is constrained by p_H and T_H. The set of feasible combinations for the transcritical CO_2 components is slightly increased as the VHC constraint is moved towards lower ammonia mass fractions. Further, it should be noted that although the VHC and low pressure constraints have moved significantly towards lower x_r the vapour ammonia mass fraction constraint actually moved slightly towards higher x_r allowing fewer solutions to satisfy this constraint.

Fig. 4 (c) has a heat supply temperature of 150 °C. Here it is seen that no combinations that satisfy the COP constraint also satisfy the constraint of T_H <170 °C. Thus, neither standard refrigeration nor high pressure NH_3 components are applicable at a heat supply temperature of 150 °C.

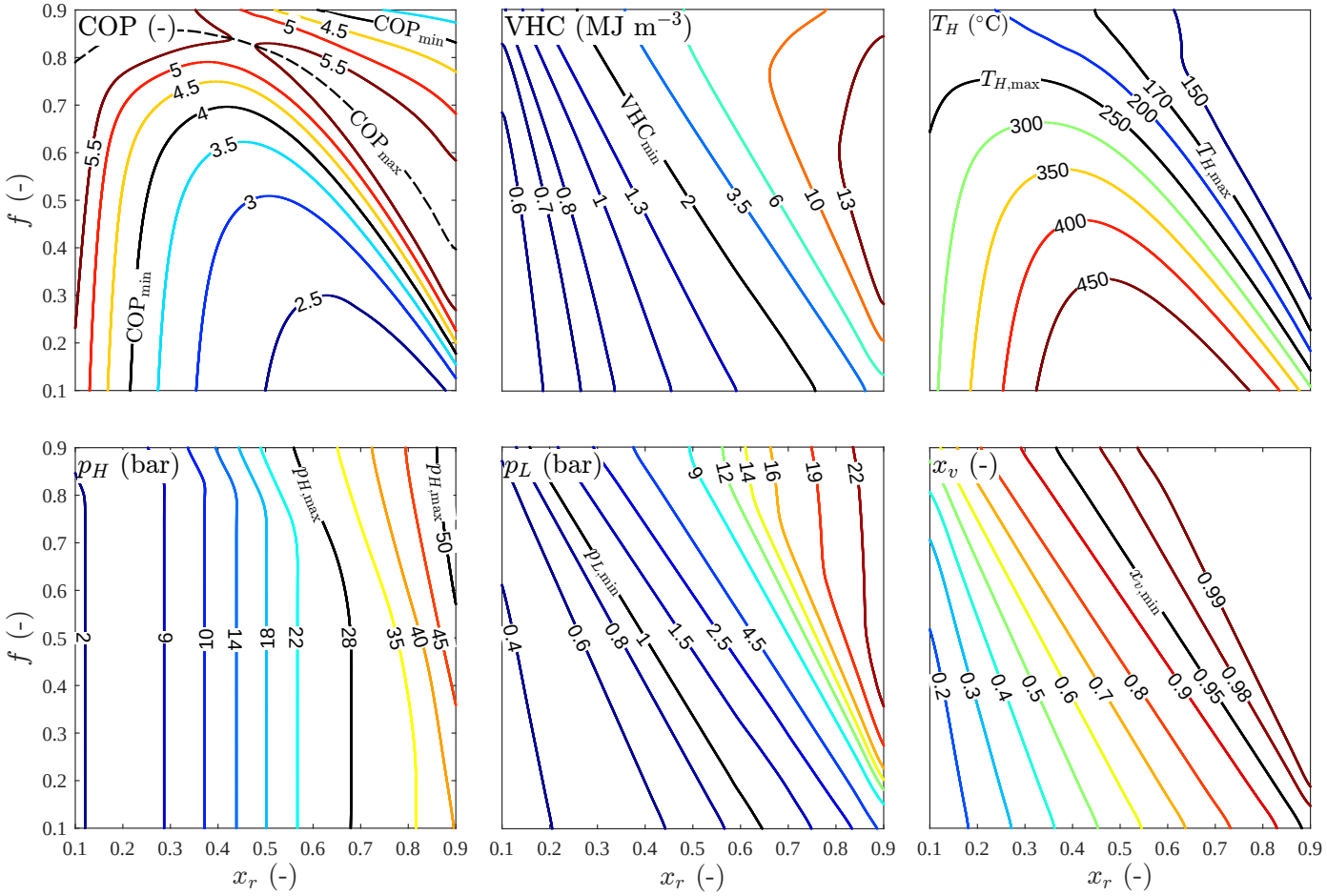

Figure 2: COP, VHC, compressor discharge temperature, T_H, high pressure, p_H, low pressure, p_L, and vapour ammonia mass fraction, x_v, as a function of the circulation ratio, f, and the ammonia mass fraction, x_r. Heat supply temperature $T_{\text{sink,out}}$ = 100 °C.

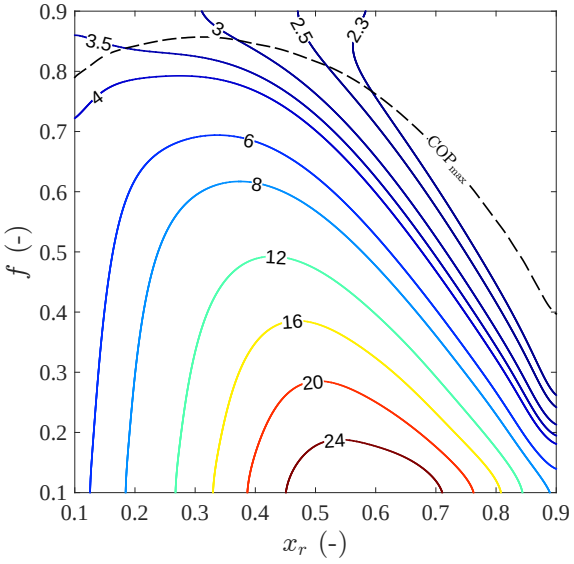

Figure 3: Pressure ratio, PR, as a function of the circulation ratio, f, and the ammonia mass fraction, x_r. Heat supply temperature $T_{\text{sink,out}}$ = 100 °C.

The VHC constraint is no longer present due to the high temperature of the heat source and consequently high desorber pressure. This again causes the set of feasible combinations for transcritical CO_2 components to expand. This set is only constrained by T_H and COP.

Fig. 4 (d) has a heat supply temperature of 175 °C. Here, for the first time the high pressure constraint for transcritical CO_2, p_H<140 bar, is present. The set of the feasible combinations is reduced compared to a heat supply temperature of 150 °C. The set is constrained by T_H, COP and p_H.

It should be noted that the increased heat supply temperature attained by the use of the transcritical CO_2 components is only possible because of the increased tolerance on the compressor discharge temperature. As seen in Fig. 4 (c) and 4 (d) a design that keeps the compressor discharge temperature below 170 °C is not possible. Hence, judging from Fig. 4, if the transcritical CO_2 compressor cannot be modified to sustain these temperatures, these components cannot attain higher supply temperatures than the high pressure NH_3 components. Further, it is seen that if the standard refrigeration and high pressure NH_3 compressors are modified to sustain 250 °C compressor discharge temperature and vapour ammonia mass fractions below 0.95 these can also attain heat supply temperatures up to

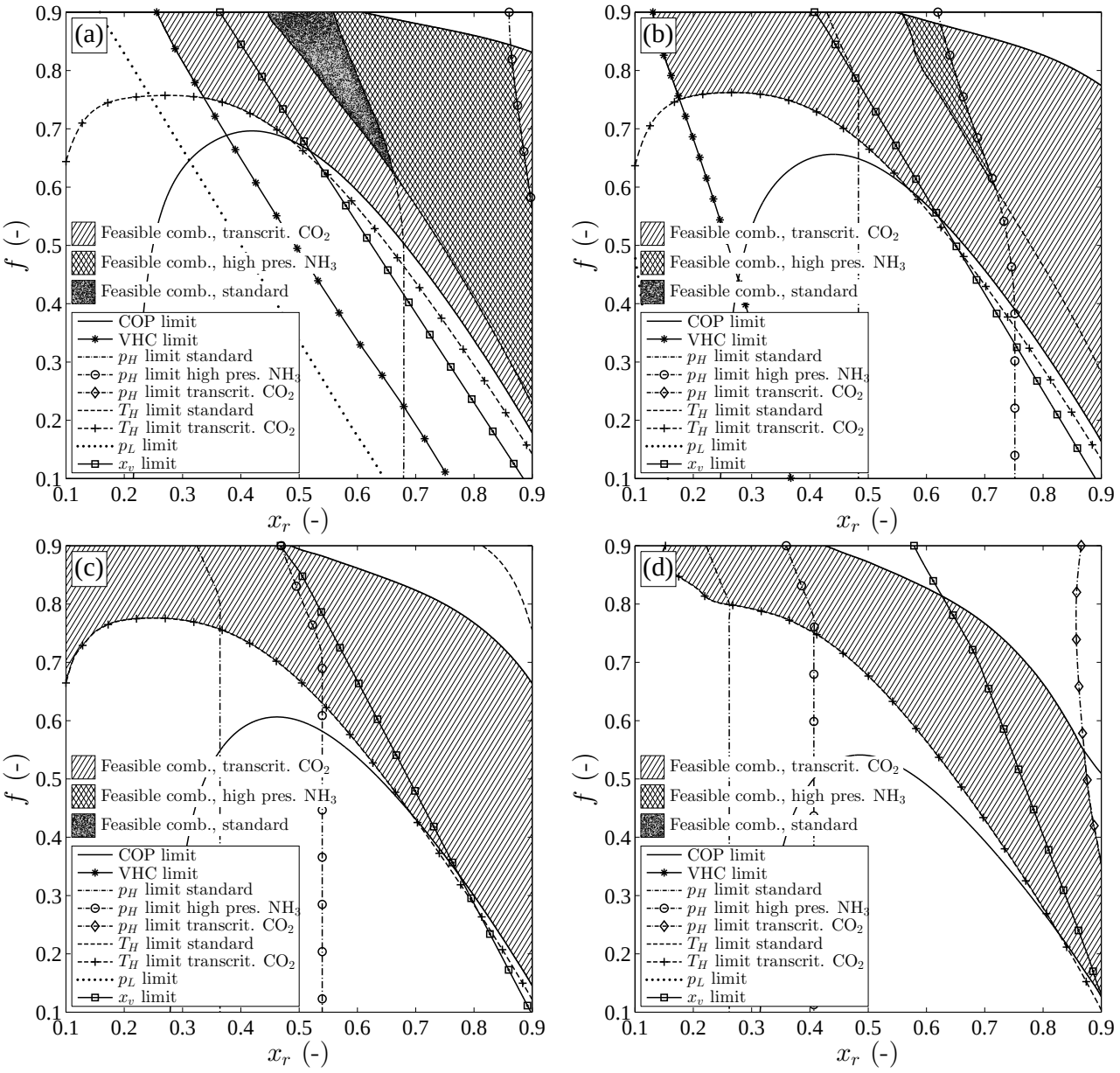

Figure 4: Feasible combinations of the circulation ratio, f, and the ammonia mass fraction, x_r, for standard, high pressure NH_3 and transcritical CO_2 components. Heat supply temperature (a): $T_{\text{sink,out}}$ = 100 °C, (b): $T_{\text{sink,out}}$ = 125 °C, (c):$T_{\text{sink,out}}$ = 150 °C, (d): $T_{\text{sink,out}}$ = 175 °C

175 °C although the set of feasible combinations of x_r and f is considerably smaller.

3.3. Maximum heat supply temperature

To get a more detailed view of the temperature levels that can be achieved by the different components, the maximum heat supply temperature was derived. The maximum heat supply temperature was defined as the temperature level at which no combinations of x_r and f result in a feasible solution.

Fig. 5 shows the maximum heat supply temperature for all three component types with a compressor discharge temperature constraint of both $T_{H,\text{max}}$ = 170 °C and $T_{H,\text{max}}$ = 250 °C and with and without the vapour ammonia mass fraction constraint. As seen, for $T_{H,\text{max}}$ = 170 °C and $x_{v,\text{min}}$ = 0.95 a maximum heat supply temperature of 111 °C can be attained with 28 bar components, 129 °C with 50 bar components and 147 °C with 140 bar components. Removing only the vapour ammonia mass fraction constraint does not lead to a further increase in attainable temperatures. Increasing only $T_{H,\text{max}}$ to 250 °C increases the maximum temperature to 127 °C, 149 °C and 187 °C for the respective pressure constraints.

As seen the largest increase in maximum heat supply temperature is attained when increasing $T_{H,\text{max}}$ to 250 °C and simultaneously removing the vapour ammonia mass fraction constraint. This allows temperatures up to 182 °C, 193 °C and 223

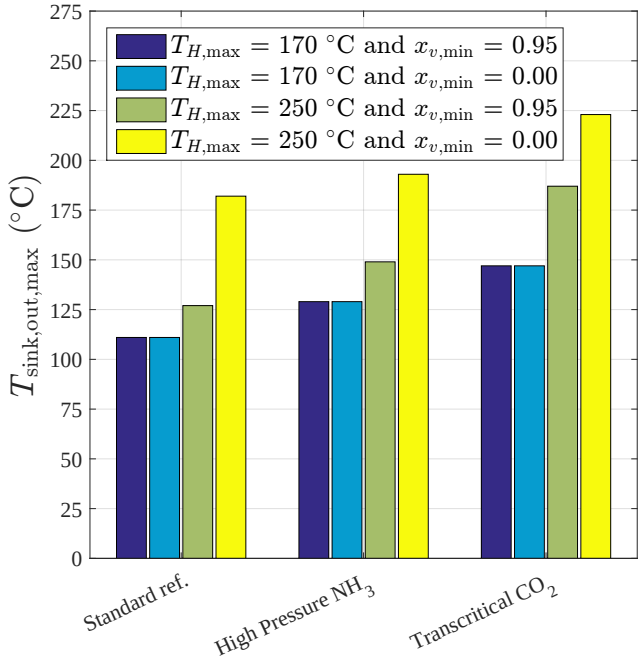

Figure 5: Maximum attainable heat supply temperature for the three investigated component types. Two maximum compressor discharge temperatures are imposed. Further, $T_{\text{sink,out,max}}$ is presented with and without the vapour ammonia mass fraction constraint.

°C for the respective pressure constraints.

The use of high pressure NH_3 and transcritical CO_2 components with a compressor discharge temperature constraint of 170 °C could still be advantageous as the increased number of feasible solutions could lead to designs with higher efficiency or low investment cost or even both. To assess this, thermo-economic analysis may be performed (Bejan et al., 1996).

3.4. Sensitivity of the component performance parameters

The results presented above are all derived with constant component inputs to the thermodynamic model. The sensitivity of these assumed values on the constrained design parameters has been evaluated at a heat supply temperature of $T_{\text{sink,out}}$ = 100 °C (Fig. 6) and $T_{\text{sink,out}}$ = 175 °C (Fig. 7), both with an ammonia mass fraction of x_r = 0.8 and a circulation ratio of f = 0.6. The sensitivity on the COP (a), VHC (b), high pressure, p_H, (c), low pressure (d), compressor discharge temperature, T_H, (e) and the vapour ammonia mass fraction, x_v, (f) is shown.

As seen the highest sensitivity on the COP is caused by the compressor electrical and isentropic efficiency. The assumed electrical efficiency of η_e = 0.9 should be attainable by most electrical motors, a reduction of 10% might happen over time thus leading to a reduction of COP of approximately 0.7. The isentropic efficiency, assumed at η_{is} = 0.75 would be significantly dependent on the applied compressor and its characteristics. A reduction of the isentropic efficiency up to 50% is not unlikely which leads to a significant reduction of COP by approximately 2. This should be avoided by choosing an appropriate compressor. The second highest influence is from the absorber and desorber pinch point temperature difference of which the absorber influence is slightly higher than that of the desorber for $T_{\text{sink,out}}$ = 175 °C while they are close to identical for $T_{\text{sink,out}}$ = 100 °C. The third highest influence is from the IHEX, it is seen that a reduction of the IHEX effectiveness of 50% results in a reduction of COP of approximately 1. The pump isentropic and electrical efficiency is seen to have a higher influence on the COP at $T_{\text{sink,out}}$ = 175 °C than at $T_{\text{sink,out}}$ = 100 °C. The gas cooler effectiveness is seen to have a minor influence on the COP at $T_{\text{sink,out}}$ = 175 °C while the influence at $T_{\text{sink,out}}$ = 100 °C is negligible.

The highest influence on the VHC is from the volumetric efficiency of the compressor, hence a reduction of the volumetric efficiency from the assumed η_{vol} = 0.90 causes a large decrease of the VHC. Reducing the compressor isentropic efficiency causes an increase in VHC, as a reduction of the isentropic efficiency causes less mass flow rate for the same heat output as the reduced isentropic efficiency increases the compressor discharge temperature. This, however causes a severe reduction of the COP. At $T_{\text{sink,out}}$ = 100 °C the VHC is positively influenced by a reduction of the desorber pinch point temperature difference, while it is almost insensitive to the absorber pinch point temperature difference at $T_{\text{sink,out}}$ = 175 °C. For $T_{\text{sink,out}}$ = 175 °C the VHC is almost equally influenced by the absorber and desorber pinch point temperature differences. A reduction of the IHEX effectiveness results in a decrease of the VHC, this influence is higher at $T_{\text{sink,out}}$ = 175 °C than at $T_{\text{sink,out}}$ = 100 °C. As for the COP the gas cooler effectiveness mainly influences the VHC at the high temperature. A reduction of ε_{GC} gives a reduction of the VHC. For both temperature levels the VHC is insensitive to a change in the pump isentropic and electrical efficiency.

The highest influence on the high pressure is from the absorber pinch point temperature difference while there is only a small influence from the desorber temperature difference. The second highest influence is from the compressor isentropic efficiency. A reduction of this leads to a reduction of the high pressure due to the increased compressor discharge temperature. This moves the pinch point further downstream in the heat exchanger resulting in the reduced pressure. A reduction of the IHEX effectiveness causes an increase in the needed high pressure for both $T_{\text{sink,out}}$ = 100 °C and $T_{\text{sink,out}}$ = 175 °C, while the gas cooler effectiveness mainly causes this behaviour for $T_{\text{sink,out}}$ = 175 °C.

As seen the main sensitivity on the low pressure stems from the desorber pinch point temperature difference. This is followed by the IHEX effectiveness which, especially for $T_{\text{sink,out}}$ = 175 °C has some effect on the low pressure. Further, the compressor isentropic efficiency has a minor influence on the low pressure. The low pressure is insensitive to the remaining inputs.

The compressor discharge temperature is mainly influenced by the isentropic efficiency. The second highest influence is from the absorber pinch point temperature difference followed by the desorber temperature difference. Both increase the compressor discharge temperature due the increased pressure ratio over the compressor. A reduction of the IHEX effectiveness

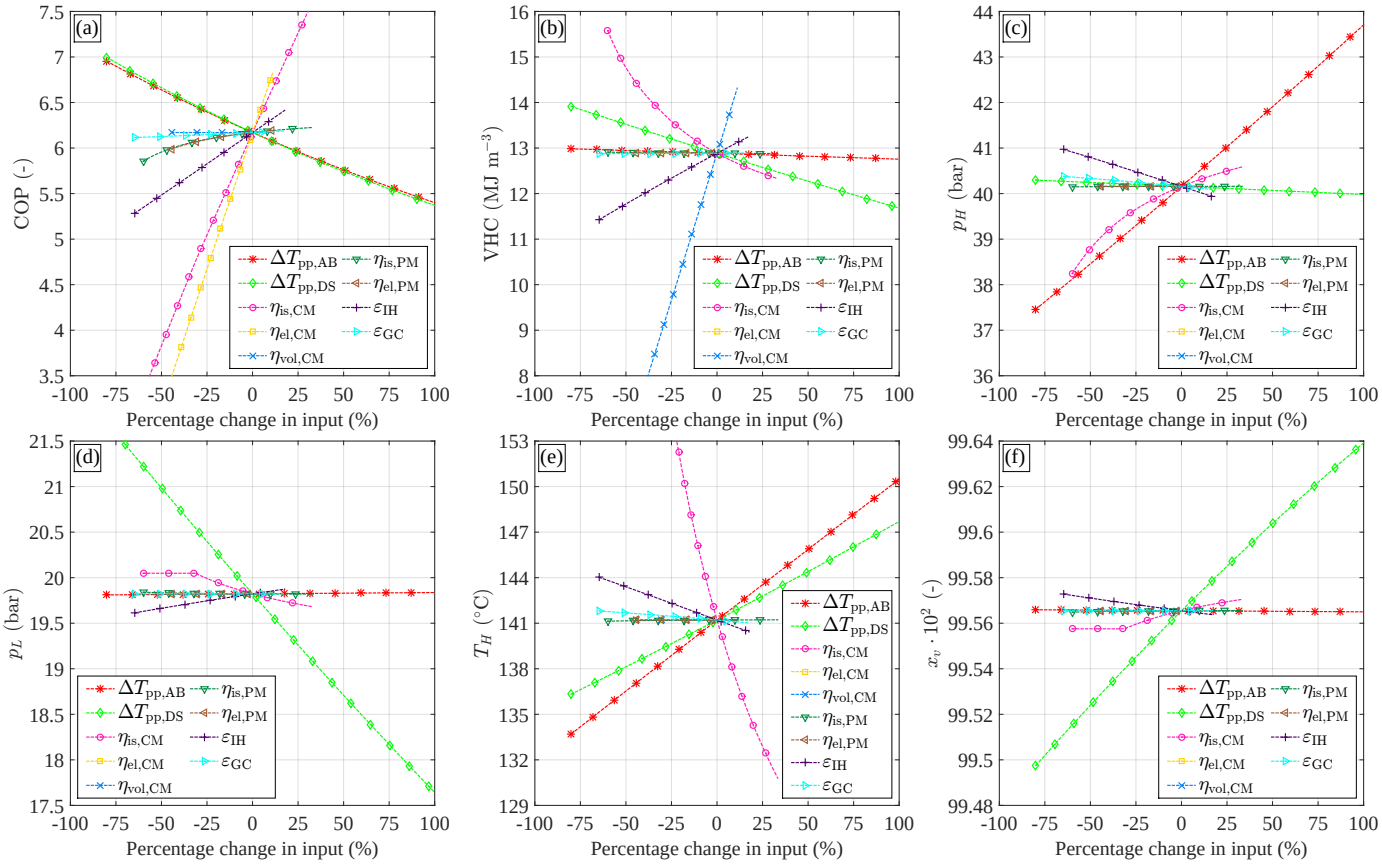

Figure 6: Sensitivity of the component inputs on the design constraints. (a): COP, (b): VHC, (c): p_H, (d): p_L, (e): T_H and (f): x_v. Heat supply temperature of: $T_{\text{sink,out}}$ = 100 °C, ammonia mass fraction of: x_r = 0.8 and circulation ratio of: f = 0.6

causes an increased compressor discharge temperature for both $T_{\text{sink,out}}$ = 100 °C and $T_{\text{sink,out}}$ = 175 °C, while the gas cooler effectiveness mainly causes this behaviour for $T_{\text{sink,out}}$ = 175 °C.

From Fig. 6 (f) and 7 (f) it is seen that the vapour ammonia mass fraction is generally insensitive to the variation of component inputs. The maximum variation of x_v is ±0.1% for $T_{\text{sink,out}}$ = 100 °C and ±0.4% for $T_{\text{sink,out}}$ = 175 °C. However, as seen from Fig. 2, x_v is close to constant for the point x_r = 0.8 and f = 0.6. Hence, the sensitivity may be larger for other combinations of x_r and f in which the x_v is less constant.

4. Discussion

Brunin et al. (1997) evaluated the HACHP at rich ammonia mass fractions of 0.25, 0.35 and 0.45 and a constant concentration difference of 0.10 between the rich and lean solution. This showed that heat supply temperatures up to 140 °C can be achieved with a high pressure constraint of 20 bar. This however does not include a constraint on the compressor discharge temperature. Ommen et al. (2011) evaluated the HACHP at x_r of 0.7 and 0.9 and a constant source glide of 10 K. The high pressure constraint was 50 bar and the compressor discharge temperature constraint was 160 °C. Here the maximum supply temperature was found to be 125 °C. This is in good agreement with results of the present study.

From Fig. 4 it is seen that if the constraint on the compressor discharge temperature and vapour ammonia mass fraction are not considered, as done by Brunin et al. (1997), supply temperatures of 182 °C arepossible for standard equipment. This again proves the importance of evaluating all combinations x_r and f. Further, it is shown that even when considering the compressor discharge temperature constraint the application of high pressure NH_3 and transcritical CO_2 components as well as an evaluation of all combinations of x_r and f, have expanded the HACHP working domains presented by Brunin et al. (1997) and Ommen et al. (2011) to cover heat supply temperatures up to 182 °C.

In general the compressor discharge temperature is shown to be the dominating constraint when assessing the HACHP applicability for high temperature design. This could be reduced by implementing a two-stage compression or an oil cooled compressor. Here it is important that the heat removed in the intercooler and compressor cooler is utilized to heat either the lean solution or the heat sink, otherwise this will lead to a reduction of the COP despite of the reduced compressor work.

Nevertheless, the compressor discharge temperature will set the upper limit of the heat supply temperature. This can be concluded only from the second law as this dictates a positive temperature difference in the gas cooler and thus $T_H > T_{\text{sink,out}}$. Hence, if the constraint of 170 °C on the compressor discharge

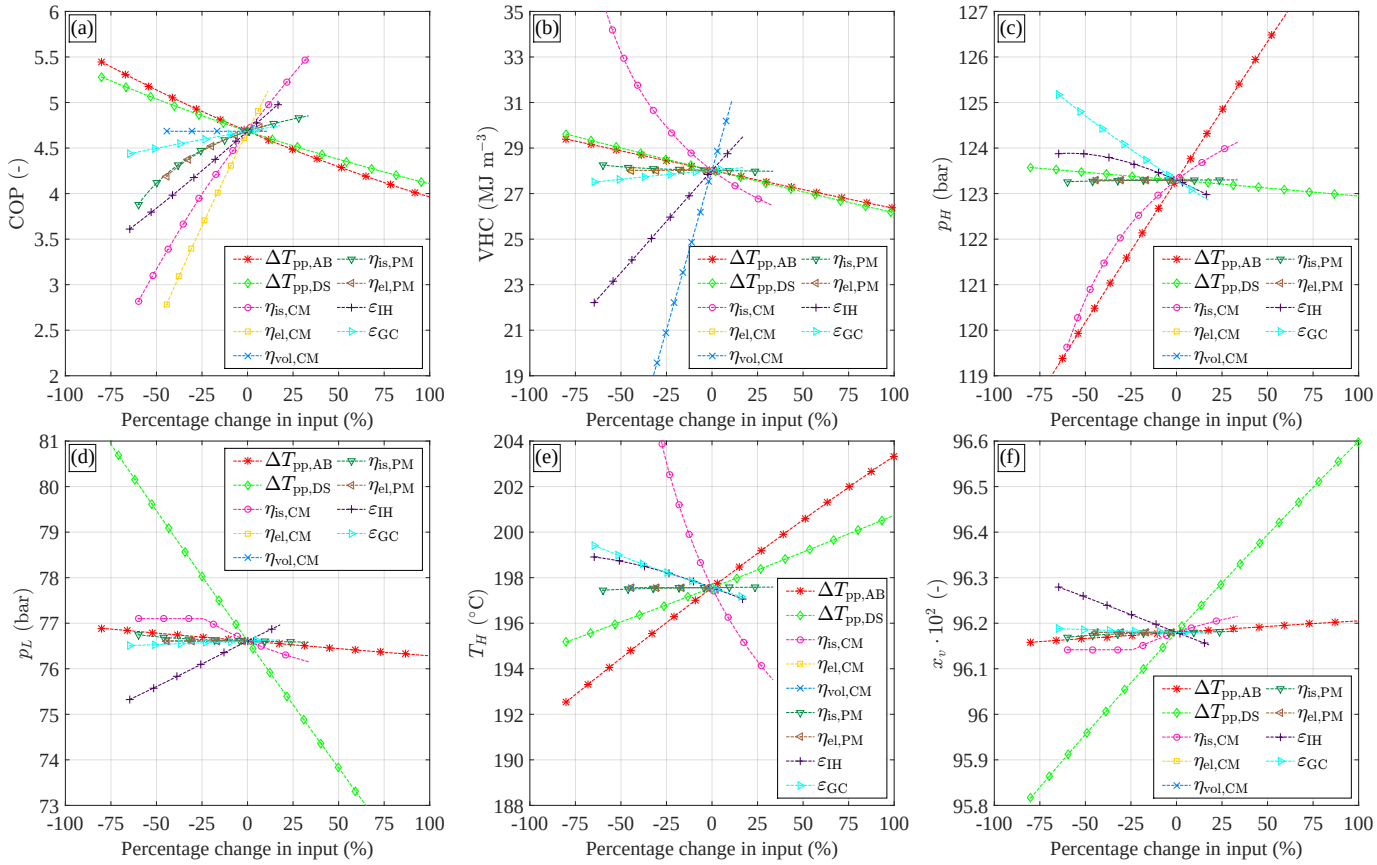

Figure 7: Sensitivity of the component inputs on the design constraints. (a): COP, (b): VHC, (c): p_H, (d): p_L, (e): T_H and (f): x_v. Heat supply temperature of: $T_{\text{sink,out}} = 175$ °C, ammonia mass fraction of: $x_r = 0.8$ and circulation ratio of: $f = 0.6$

temperature cannot be increased then maximum heat supply temperature will never be higher than this.

The vapour ammonia mass fraction is also shown to influence the attainable temperatures, however to which extent the compression of a water-rich ammonia-water vapour poses a real issue for ammonia compressors is uncertain. From a thermodynamic perspective compression of such vapour is not an issue as long as a feasible COP and VHC are attained. Whether there exist material constraints that limit the allowable water content should be further investigated.

The vapour ammonia mass fraction could be increased by installing rectification in the suction line or by using a falling film desorber in which the desorbed vapour is in counter flow with the desorbing liquid, thereby reducing the vapour outlet temperature and consequently increasing the vapour ammonia mass fractions. However, both solutions will introduce irreversibilities to the system and will thus reduce the COP.

5. Conclusion

Results show that all constrained design parameters are highly influenced by the choice of rich ammonia mass fraction and circulation ratio. This emphasises the importance of finding a suitable combination. At circulation ratios below 0.5 and rich ammonia mass fractions between 0.2-0.8 a set of combinations induce a substantial increase in pressure ratio. Consequently reducing the COP and increasing the compressor discharge temperature, designing the HACHP within this set of combinations is therefore not recommended.

Three sets of design constraints have been applied to the choice of rich ammonia mass fraction and circulation ratio. This shows that the HACHP using standard refrigeration components can attain heat supply temperatures of 111 °C with an unmodified compressor and 127 °C if the compressor is modified to sustain higher discharge temperatures. If the compressor is not constrained by the vapour ammonia mass fraction, temperatures of 182 °C can be attained. High pressure NH_3 components increase this to 129 °C, 149 °C and 193 °C. The set of feasible combinations for the unmodified standard refrigeration components and the unmodified high pressure NH_3 components is constrained mainly by the high pressure and the compressor discharge temperature.

Heat supply temperatures of either 187 °C or 223 °C is possible using transcritical CO_2 components, depending on the allowable compressor discharge temperature. If the vapour ammonia mass fraction is constrained, as for the NH_3 compressors, the maximum heat supply temperature for the transcritical CO_2 components is reduced to 147 °C.

The dominating constraints when evaluating the maximum heat supply temperature are the high pressure, the compres-

sor discharge temperature and the vapour ammonia mass fraction. If the attainable heat supply temperature of the HACHP is to be increased it is not sufficient to only increase allowable pressure, the allowable compressor discharge temperature and vapour ammonia mass fraction must also be increased.

The sensitivity analysis shows that the highest influence on the high pressure stems from the absorber pinch point temperature difference, while the highest influence on the compressor discharge temperature stems from the isentropic efficiency of the compressor. On the other hand vapour ammonia mass fraction is insensitive to the component inputs.

The use of a two stage compression and oil cooled compressors will reduce the compressor discharge temperature and should be evaluated for high temperature HACHP development.

Acknowledgements

This research project is financially funded by EUDP (Energy Technology Development and Demonstration). Project title: "Development of ultra-high temperature hybrid heat pump for process application", project number: 64011-0351

References

Altenkirch, E., 1950. Kompressionskältemachine mit lösungskreislauf. Kältetechnik 10, 251–259, 11, 279–284, 12, 310–315.

Bejan, A., Tsatsaronis, G., Moran, M.J., 1996. Thermal Design and Optimization. Wiley, New York.

Berntsson, T., Hultén, M., 1999. The compression/absorption cycle – influence of some major parameters on COP and a comparison with the compression cycle. Int. J. Refrigeration 22, 91–106. doi:10.1016/S0140-7007(98)00047-4

Berntsson, T., Hultén, M., 2002. The compression/absorption heat pump cycle - conceptual design improvements and comparisons with the compression cycle. Int. J. Refrigeration 25, 487–497. doi:10.1016/S0140-7007(02)00014-2

Brunin, O., Feidt, M., Hivet, B., 1997. Comparison of the working domains of some compression heat pumps and a compression-absorption heat pump. Int. J. Refrigeration 20, 308–318. doi:10.1016/S0140-7007(97)00025-X

Itard, L.C.M., Machielsen, C.H.M., 1994 Considerations when modelling compression/resorption heat pumps. Int. J. Refrigeration 17, 453–460. doi:10.1016/0140-7007(94)90005-1

Lorenz, H., 1894. Beiträge zur Beurteilung von Kühlmaschinen. Z VDI 38, 62–68, 98–103, 124–130.

MATLAB 2015a, MathWorks, 2015, `http://www.mathworks.se /products/matlab/`.

Modi, A., Haglind, F., 2015. Thermodynamic optimisation and analysis of four Kalina cycle layouts for high temperature applications. Appl. Therm. Eng. 76, 196–205. doi:10.1016/j.applthermaleng.2014.11.047

Nekså, P., Rekstad, H., Zakeri, G.R., Schiefloe, P.A., 1998. CO_2-heat pump water heater: characteristics, system design and experimental results. Int. J. Refrigeration 21, 172–179. doi:10.1016/S0140-7007(98)00017-6

Ommen, T.S., Markussen, C.M., Reinholdt, L., Elmegaard, B., 2011. Thermoeconomic comparision of industrial heat pump. In: 23rd IIR International Congress of Refrigeration, August 21 - 26 - Prague, Czech Republic, Paper ID: 532.

Osenbrück, A., 1895, Verfahren zur Kälteerzeugung bei Absorptionsmaschinen. Deutsches Reichspatent, [DRP 84084].

Rane, M.V. Radermacher, R., 1992. Feasibility study of a two-stage vapour compression heat pump with ammonia-water solution circuits: experimental results. Int. J. Refrigeration 16, 258–264. doi:10.1016/0140-7007(93)90078-M

Rane, M.V. Amrane, K., Radermacher, R., 1993. Performance enhancement of a two-stage vapour compression heat pump with solution circuits by eliminating the rectifier. Int. J. Refrigeration 16, 247–257. doi:10.1016/0140-7007(93)90077-L

REFPROP 9.1, National Institute for Standards and Technology, MATLAB Interface, in: MatLabApplications 2013, `http://www.boulder.nist.gov/div838/theory/refprop/Frequently_asked_questions.htm#`.

Stokar, M., Trepp, C.H., 1987. Compression heat pump with solution circuit Part 1 : design and experimental results. Int. J. Refrigeration 10, 87–96. doi:10.1016/0140-7007(87)90026-0

Tillner-Roth, R., Friend, D.G., 1998. A Helmholtz Free Energy Formulation of the Thermodynamic Properties of the Mixture {Water + Ammonia}. J. Phys. Chem. Ref. Data 27, 63–94. doi:10.1063/1.556015

Zamjlrescu, C., 2009. Modeling and optimization of an ammonia water compression resorption heat pumps with wet compression. Trans. Can. Soc. Mech. Eng 33, 75–88.

Zheng, N., Weidong, S., Zhao, L., 2013. Theoretical and experimental investigations on the changing regularity of the extreme point of the temperature difference between zeotropic mixtures and heat transfer fluid. Energy 55, 541–552. doi:10.1016/j.energy.2013.02.029

Åhlby, L., Berntsson, T., Hodgett, D., 1991. Optimization study of the compression/absorption cycle. Int. J. Refrigeration 14, 16–23. doi:10.1016/0140-7007(91)90017-B